ACS OMEGA

Open Access

This article is licensed under CC-BY-NC-ND 4.0

http://pubs.acs.org/journal/acsodf

Article

Efficient Iodine Uptake of Ultra Thermally Stable Conjugated Copolymers Bearing Biaceanthrylenyl Moieties and Contorted Aromatic Units Using a [3 + 2] Palladium-Catalyzed Cyclopolymerization Reaction

Noorullah Baig, Suchetha Shetty, Rupa Bargakshatriya, Sumit Kumar Pramanik, and Bassam Alameddine*

Cite This: *ACS Omega* 2023, 8, 43227−43235

Read Online

ACCESS | Metrics & More | Article Recommendations | Supporting Information

ABSTRACT: A novel series of copolymers made from alternating aromatic surrogates with contorted and spiro compounds, denoted as **BCP1−3**, was successfully synthesized employing a palladium-catalyzed one-pot [3 + 2] cyclopentannulation reaction. The resulting copolymers **BCP1−3**, which were isolated in high yields, exhibited weight-average molecular weights (M_w) ranging from 11.0 to 61.5 kg mol^{-1} (kDa) and polydispersity index (M_w/M_n) values in the range of 1.7 and 2.0, which suggest a narrow molecular weight distribution, thus indicating the formation of uniform copolymer chains. Investigation of the thermal properties of **BCP1−3** by thermogravimetric analysis disclosed outstanding stability with 10% weight loss temperature values reaching 800 °C. Iodine adsorption tests revealed remarkable results, particularly for **BCP2**, which demonstrated a strong affinity toward iodine reaching an uptake of 2900 mg g^{-1}. Additionally, recyclability tests showcased the effective regeneration of **BCP2** after several successive iodine adsorption−desorption cycles.

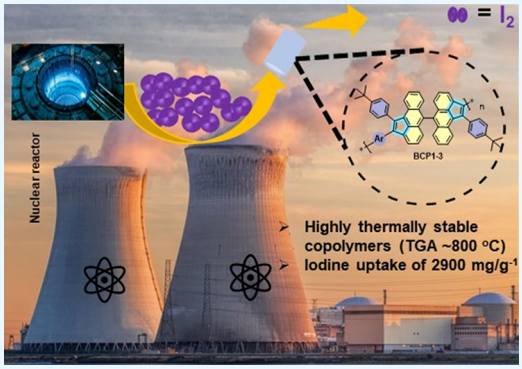

1. INTRODUCTION

Conjugated polymers emerged as a fascinating family of materials which have revolutionized various fields of science and technology[1−3] because of their exceptional optical and electronic properties bestowed with their versatile processability, thus allowing for their use across a myriad of applications, notably, optoelectronic devices and energy storage and conversion.[4−7] These applications encompass organic photodetectors and photovoltaics (OPDs and OPVs),[8,9] light-emitting diodes (OLEDs),[10] and field-effect transistors (OFETs).[11,12]

Conjugated copolymers made from [3 + 2] cyclopolymerization reactions have gotten noticeable interest as potential components for organic electronics[13,14] as they are characterized by unique structural features where the cyclopentannulated rings are incorporated into the backbone of the conjugated chains,[15,16] thus improving the polymers' structural rigidity and planarity, consequently enhancing the charge delocalization along the macromolecular chain.[17] Several studies have reported the synthesis of cyclopentannulated copolymers with remarkable optical and electrochemical properties for applications in optoelectronics.[14,18−20] It is noteworthy that our group has been the first to report the synthesis of specially designed cyclopentannulated copolymers as adsorbent materials revealing high uptake capacity of iodine and toxic organic dyes.[13,21]

Nuclear power has proven as a reliable mega source of energy but whose management and safe disposal of radioactive waste remain a chief challenge to overcome.[22] Among the primary constituents of nuclear waste are iodine radioisotopes, namely, ^{125}I, ^{129}I, ^{131}I, and ^{133}I which are volatile and hazardous substances interfering in human metabolic processes.[23−25] Therefore, there is a dire need to find effective solutions for a proper removal of these radioactive halides.[26] Adsorption has arisen as a viable technology to capture iodine from gases and liquids leading to the investigation of a wide range of adsorbent materials, e.g., zeolites,[22] metal−organic frameworks (MOFs),[27] covalent-organic polymers (COPs),[28,29] covalent-organic frameworks (COFs),[26,30] metalorganic copolymers,[31,32] and porous organic polymers.[33,34] Although these materials offer several advantages, such as the simplicity of the

Received: September 17, 2023
Revised: October 18, 2023
Accepted: October 19, 2023
Published: November 1, 2023

© 2023 The Authors. Published by American Chemical Society

required equipment and ease of operation besides their cost-effectiveness and recyclability, the development of adsorbents with high iodine uptake but which can sustain the extremely harsh conditions encountered in a fission nuclear reactor remains the main challenge.[35]

We disclose herein the synthesis of conjugated copolymers **BCP1−3** using a versatile [3 + 2] cyclopentannulation reaction and in which different contorted aryl dialkynyl synthons **2a−c** were reacted with the starting material 10,10′-dibromo-9,9′-bianthracene (**3**) yielding the desired copolymers. **BCP1−3** structures were confirmed by nuclear magnetic resonance (NMR), Fourier-transform infrared (FTIR), and UV−visible absorption and emission spectroscopies. Thermogravimetric analysis (TGA) of the hitherto mentioned copolymers unveiled their superior thermal stability with 10% mass loss temperatures attaining values up to 800 °C. All the target copolymers proved high iodine uptake capacities reaching 2900 mg g^{-1} for **BCP2**.

2. MATERIAL AND METHODS

2.1. Materials. The chemical reactions were performed in an inert environment employing dry argon. Unless otherwise noted, all the reagents were utilized as purchased from the suppliers (e.g., Merck and HiMedia). 2,7-Bis((4-(*tert*-butyl)-phenyl)ethynyl)-9,9-dimethyl-9H-fluorene (**2a**), 2,7-bis((4-(*tert*-butyl)phenyl)ethynyl)-9,9′-spirobi[fluorene] (**2b**), and 1,4-bis((4-(*tert*-butyl)phenyl) ethynyl)-9,10-dihydro-9,10-[1,2]benzenoanthracene (**2c**) were synthesized following the literature.[17,21,36] The solvents were deoxygenated by bubbling with a positive stream of dry $Ar_{(g)}$ for half an hour. Aluminum sheets covered with silica gel 60 F254 were used for thin-layer chromatography (TLC), which were revealed under an ultraviolet light source. Nuclear magnetic resonance (^{1}H: 600 MHz and ^{13}C: 150 MHz) data were collected at 25 °C using a JEOL spectrometer (model ECZ600R). $CDCl_3$ was used as a solvent, and the chemical shifts (δ) are provided in ppm and referred to tetramethylsilane (TMS). Fourier transform infrared spectra were recorded on a PerkinElmer G spectrophotometer in KBr pellets between 400 and 4000 cm^{-1}. A Shimadzu UV1800 spectrophotometer was used to record UV−vis spectra. Photoluminescence (PL) spectra were measured by using an Agilent G9800 Cary Eclipse Fluorescence spectrophotometer. The molar masses of the polymers were elucidated employing an Agilent Gel Permeation Chromatograph model 1260 Infinity II equipped with a refractive index (RI) detector and two columns (PL mixed-C) which were calibrated against a set of 12 monodisperse polystyrene (PS) standards and using tetrahydrofuran as the eluent at room temperature. TGA was performed using a Mettler Toledo Star SW 8.10 system (model number TGA/SDTA851e) analyzer to assess the polymers' stability from room temperature to 800 °C using a 10 °C/min heating rate under an inert atmosphere. Mass spectra were obtained from a Waters QTOF Micro YA263 electrospray ionization mass spectrometer.

2.2. Synthesis. *2.2.1. **BCM1** (Procedure A).* A Schlenk reactor was filled with $Ar_{(g)}$ and loaded with the following reagents: 2,7-bis((4-(*tert*-butyl)phenyl)ethynyl)-9,9-dimethyl-9H-fluorene **2a** (50 mg, 0.1 mmol, 1.0 equiv), 9-bromoanthracene **1** (56 mg, 0.22 mmol, 2.2 equiv), $Pd_2(dba)_3$ (9 mg, 10 μmol, 10 mol %), tris(o-tolyl)phosphine P(*o*-tol)$_3$ (3.0 mg, 10 μmol), KOAc (49 mg, 0.5 mmol), and LiCl (8.5 mg, 0.2 mmol). A 2 mL portion of a 1:1 DMF and toluene mixture was added to the reaction mixture, and the resulting solution was stirred at 130 °C overnight. The solvent was subsequently removed under reduced pressure, and dichloromethane (DCM) was added to the resulting mixture, followed by the extraction with a saturated solution of sodium bicarbonate (25 mL × 2). The organic layer was then washed with distilled water (50 mL × 3) before it was concentrated. The product was obtained by precipitation from ethanol and filtered under reduced pressure using a Millipore filter, followed by thorough washings with ethanol to afford a brick red solid (80 mg, 95%). ^{1}H NMR (600 MHz, $CDCl_3$, ppm): δ 8.52 (*d*, 2H, *J* = 10.9 Hz, ArH), 8.10−8.04 (*m*, 6H, ArH), 7.90 (*d*, 2H, *J* = 6.6 Hz, ArH) 7.82 (*t*, 2H, *J* = 7.5 Hz, ArH), 7.66−7.63 (*m*, 2H, ArH), 7.56 (*m*, 2H, ArH), 7.48−7.47 (*m*, 4H, ArH), 7.41−7.30 (*m*, 10H, ArH),1.38 (*s*, 6H, $-CH_3$),1.30 (*s*, 18H, $-CH_3$). ^{13}C NMR (150 MHz, $CDCl_3$, ppm): δ 153.98, 149.54, 140.76, 139.99, 139.78, 138.13, 137.61, 136.72, 135.08, 134.59, 132.48, 130.71, 130.43, 130.10, 129.35, 128.93, 128.22, 127.35, 126.55, 125.88, 125.13, 124.84, 124.50, 119.85, 46.44, 34.63, 31.59. ESI-MS; Calculated for $M^{\cdot+}$ $C_{67}H_{54}$: 859.40; found 859.40.

*2.2.2. Synthesis of **BCM2**.* **BCM2** was prepared following procedure A with 2,7-bis((4-(*tert*-butyl)phenyl)ethynyl)-9,9′-spirobi[fluorene] **2b**, (50 mg, 0.08 mmol, 1.0 equiv), 9-bromoanthracene **1** (45 mg, 0.18 mmol, 2.2 equiv), $Pd_2(dba)_3$ (7.3 mg, 8.0 μmol, 10 mol %), P(*o*-tol)$_3$, (2.4 mg, 8.0 μmol), KOAc (39 mg, 0.4 mmol), and LiCl (6.7 mg, 0.16 mmol) in 1 mL of a 1:1 deoxygenated mixture of DMF and toluene. Brick red solid (70 mg, 90%). ^{1}H NMR (600 MHz, $CDCl_3$, ppm): δ 8.40 (*t*, 2H, *J* = 8.5 Hz, ArH), 8.00−7.93 (*m*, 4H, ArH), 7.80 (*d*, 2H, *J* = 7.7 Hz, ArH) 7.72 (*d*, 2H, *J* = 8.4 Hz, ArH), 7.63 (*m*, 2H, ArH), 7.58−7.54 (*m*, 2H, ArH), 7.44 (*m*, 2H, ArH), 7.41−7.26 (*m*, 14H, ArH), 7.22−7.12 (*m*, 4H, ArH), 7.07−7.00 (*m*, 4H, ArH), 1.37 (*s*, 18H, $-CH_3$). ^{13}C NMR (150 MHz, $CDCl_3$, ppm): δ 149.41, 141.92, 140.83, 139.90, 137.52, 137.22, 136.33, 135.14, 134.89, 132.15, 130.55, 130.52, 130.40, 130.32, 129.94, 128.76, 128.12, 127.85, 127.71, 127.19, 126.37, 126.00, 125.73, 125.08, 124.36, 120.14, 63.56, 34.76, 31.61. ESI-MS; Calcd for $M^{\cdot+}$ $C_{77}H_{56}$: 981.66; found 981.66.

2.2.3. BCM3. **BCM3** was synthesized following procedure A with 1,4-bis((4-(*tert*-butyl)phenyl)ethynyl)-9,10-dihydro-9,10-[1,2]benzenoanthracene **2c**, (113 mg, 0.2 mmol, 1.0 equiv), 9-bromoanthracene **1** (108 mg, 0.42 mmol, 2.1 equiv), $Pd_2(dba)_3$ (18.3 mg, 0.02 mmol, 10 mol %), P(*o*-tol)$_3$, (6.0 mg, 20 μmol), KOAc (98 mg, 1.0 mmol), and LiCl (17 mg, 0.4 mmol) in a 1:1 2 mL mixture of deoxygenated DMF and toluene. Brick red solid (133 mg, 73%). ^{1}H NMR (600 MHz, $CDCl_3$, ppm): δ 8.56 (*s*, 2H, ArH), 8.14−8.06 (*m*, 10H, ArH), 7.78−7.75 (*m*, 2H, ArH) 7.44−7.39 (*m*, 6H, ArH), 7.32 (*m*, 6H, ArH), 7.13 (*s*, 2H, ArH), 7.01−6.97 (q, 2H, *J* = 10.0 Hz, ArH), 6.78−6.73 (*m*, 4H, ArH), 1.35 (*s*, 18H, $-CH_3$). ^{13}C NMR (150 MHz, $CDCl_3$, ppm): δ 149.55, 144.89, 139.99, 138.00, 137.76, 135.10, 133.12, 132.30, 130.23, 130.04, 129.79, 128.69, 128.30, 127.38, 127.15, 126.95, 126.54, 126.36, 125.76, 125.59, 125.09, 124.63, 124.44, 124.28, 123.60, 123.36, 52.00, 34.63, 31.50. ESI-MS; Calcd for $M^{\cdot+}$ $C_{72}H_{54}$: 919.40; found 919.40.

*2.2.4. Copolymer **BCP1** (Procedure B).* 10,10′-Dibromo-9,9′-bianthracene **3** (256 mg, 0.5 mmol, 1 equiv), **2a** (253 mg, 0.5 mmol, 1 equiv), $Pd_2(dba)_3$ (46 mg, 0.05 mmol, 10 mol %), P(*o*-tol)$_3$ (23 mg, 0.075 mmol), KOAc (24 mg, 2.5 mmol), and LiCl (42 mg, 1.0 mmol) were charged in a Schlenk reactor under a reflux of Ar followed by the addition of 10 mL of a 1:1 DMF/toluene. The reaction mixture was stirred at 130 °C for

https://doi.org/10.1021/acsomega.3c07108
ACS Omega 2023, 8, 43227−43235

6 days before evaporation of the solvent under reduced pressure. The resulting mixture was then dissolved in methylene dichloride before extraction with $NaHCO_{3(sat.)}$ (50 mL × 2). The organic layer was washed with distilled water (100 mL × 3) before it was concentrated and subsequently precipitated by slowly adding acetone. The brick red solid was filtered and washed thoroughly with water, methanol, and acetone and then dried under vacuum to afford a brick red solid (400 mg, 94%). ^{1}H NMR (600 MHz, $CDCl_3$, ppm): δ 8.14 (*brm*, 2H, ArH), 7.91 (*br*, 2H, ArH), 7.65 (*bm*, 4H, ArH) 7.39 (*br*, 10H, ArH), 7.32 (*br*, 6H, ArH), 7.12 (*br*, 4H, ArH), 1.44 (*s*, 6H, $-CH_3$), 1.34 (*s*, 18H, $-CH_3$). ^{13}C NMR (150 MHz, $CDCl_3$, ppm): δ 154.12, 149.72, 140.80, 140.19, 138.28, 136.78, 136.36, 135.18, 134.97, 132.40, 131.46, 130.59, 130.12, 129.52, 128.25, 127.71, 127.01, 126.03, 125.49, 125.17, 125.01, 120.05, 46.94, 34.85, 31.67, 31.02; GPC traces: M_w = 61550 Da, M_n = 30390 Da, $Đ$ = 2.0; FTIR (KBr, cm^{-1}): 3064, 2956, 1680, 1441, 829; UV−vis: (THF, 10^{-6} M), λ_{max} [nm] = 380, 434, 452 and 520.

*2.2.5. Copolymer **BCP2**.* **BCP2** was made using procedure B with 10,10′-dibromo-9,9′-bianthracene **3** (256 mg, 0.5 mmol, 1 equiv), **2b** (314 mg, 0.5 mmol, 1 equiv), $Pd_2(dba)_3$ (46 mg, 0.05 mmol, 10 mol %), P(*o*-tol)$_3$ (23 mg, 0.075 mmol), KOAc (24 mg, 2.5 mmol), and LiCl (42 mg, 1.0 mmol) in 10 mL of a 1:1 DMF/toluene mixture. Brick red solid (415 mg, 85%). ^{1}H NMR (600 MHz, $CDCl_3$, ppm): δ 7.96−7.76 (*m*, 8H, ArH), 7.56−7.41 (*bm*, 6H, ArH), 7.33−7.27 (*bm*, 10H, ArH), 7.21−7.15 (*bm*, 6H, ArH), 7.05−6.98 (*br*, 6H, ArH), 1.36 (*s*, 18H, $-CH_3$); ^{13}C NMR (150 MHz, $CDCl_3$, ppm): δ 149.50, 146.29, 142.02, 139.99, 137.71, 135.01, 132.17, 129.98, 128.72, 128.49, 127.96, 127.82, 127.50, 127.35, 127.04, 126.33, 126.11, 125.87, 125.14, 125.13, 120.27, 120.17, 66.29, 34.68, 31.64; GPC traces: M_w = 11000 Da, M_n = 6400 Da, $Đ$ = 1.7; FTIR (KBr, cm^{-1}): 3061, 2954, 1434, 836; UV−vis: (THF, 10^{-6} M), λ_{max} [nm] = 380, 424 and 520.

*2.2.6. Copolymer **BCP3**.* **BCP3** was made employing procedure B with 10,10′-dibromo-9,9′-bianthracene **3** (256 mg, 0.5 mmol, 1 equiv), **2c** (283 mg, 0.5 mmol, 1 equiv), $Pd_2(dba)_3$ (46 mg, 0.05 mmol, 10 mol %), P(*o*-tol)$_3$ (23 mg, 0.075 mmol), KOAc (24 mg, 2.5 mmol), and LiCl (42 mg, 1.0 mmol) in 10 mL of a 1:1 DMF/toluene mixture. Brick red solid (440 mg, 96%). ^{1}H NMR (600 MHz, $CDCl_3$, ppm): δ 8.19 (*br*, 2H, ArH), 7.71−7.35 (*bm*, 16H, ArH), 6.88−6.72 (*br*, 12H, ArH) 5.92 (*br*, 2H, triptycene-CH), 1.33 (*br*, 18H, $-CH_3$). ^{13}C NMR (150 MHz, $CDCl_3$, ppm): δ 149.80, 145.59, 145.18, 140.20, 138.45, 138.00, 136.64, 136.08, 135.90, 135.12, 133.36, 132.34, 131.41, 130.43, 129.89, 129.17, 128.40, 127.58, 127.31, 127.03, 126.43, 125.97, 125.20, 124.64, 52.20, 34.67, 31.66; GPC traces: M_w = 15600 Da, M_n = 8800 Da, $Đ$ = 1.8; FTIR (KBr, cm^{-1}): 3065, 2963, 1438, 836; UV−vis: (THF, 10^{-6} M), λ_{max} [nm] = 380, 424, 450 and 520.

3. RESULTS AND DISCUSSION

3.1. Synthesis of the Prototypical Monomers. The feasibility of the reaction was tested by making three prototypical monomers synthesized, as can be noticed from Scheme 1 which describes the synthetic pathway for derivatives **BCM1−3**. These building blocks were made by reacting 2 equiv of 9-bromoanthracene **1** with each of the contorted diethynyl aryl surrogates **2a−c** using a typical cyclopentannulation reaction procedure[17] which employs a catalytic amount of $pd_2(dba)_3$ and P(o-tol)$_3$ in the presence of 5 equiv of KOAc and 2 equiv of LiCl in a deoxygenated 1:1 mixture of DMF/

Scheme 1. Synthesis of Prototypical Monomers BCM1−3

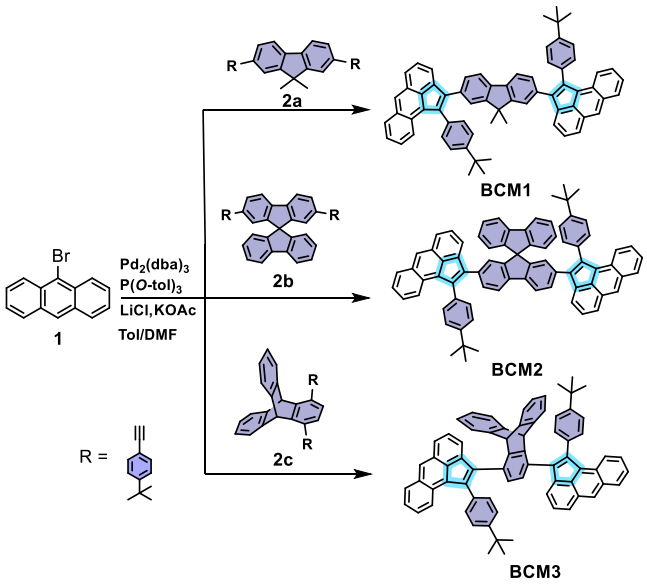

toluene at 130 °C under argon for 1 day, thus providing 73−95% of the target products in high purity, as confirmed by various analytical techniques such as NMR (^{1}H and ^{13}C), ESI-MS, and FTIR spectra (Figures S1−S3, S7−S9, S15−S20 in the Supporting Information file).

Figure 1 depicts the ^{1}H NMR spectra for each of the starting materials **1** and **2c**, against **BCM3**, where the latter clearly

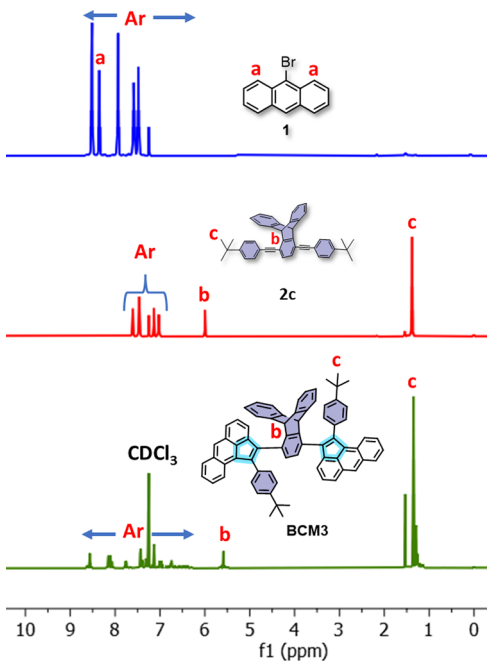

Figure 1. Comparative ^{1}H NMR spectra of **1**, **2c**, and **BCM3**.

corroborates the presence of all the desirable peaks and indicates the disappearance of those correlated to **1** and **2c**. Thus, the aromatic protons of **BCM3** were observed in the range of 8.5−6.7 ppm (see Figures 1 and S3 in Supporting Information). It is noteworthy that one of the two distinctive aromatic α-protons in 9-bromoanthracene **1** and which are detected at ∼8.3 ppm (c.f. peaks labeled **a** in Figure 1)

https://doi.org/10.1021/acsomega.3c07108
ACS Omega 2023, 8, 43227−43235

Scheme 2. Synthesis of Copolymers BCP1−3

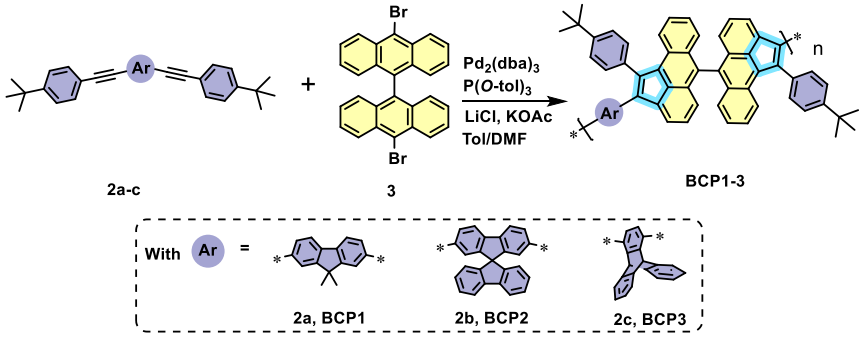

Table 1. Optimization Conditions of Copolymers BCP1-3

entry	compound[a]	yield (%)	reaction time (days)	C_M [M]	M_w (kDa)	M_n (kDa)	$Đ$
1	BCP1	98	4	1.0×10^{-1}	31.5	12.5	2.5
2	BCP1	50	4	5.0×10^{-2}	28.2	12.2	2.3
3	BCP1	40	4	2.0×10^{-1}	10.0	3.6	2.8
4	BCP1	99	6	1.0×10^{-1}	61.5	30.4	2.0
5	BCP2	85	6	1.0×10^{-1}	11.0	6.4	1.7
6	BCP3	98	6	1.0×10^{-1}	15.6	8.8	1.8

[a]$Pd_2(dba)_3$, P(*O*-tol)$_3$, LiCl, KOAC; Tol/DMF; 130 °C.

completely disappeared, while the other shifted upfield to ∼8.14 ppm in the ^{1}H NMR spectrum of **BCM3**, thus proving the successful [3 + 2] cycloaddition. Additionally, the ^{1}H NMR spectrum of **BCM3** revealed the characteristic peaks corresponding to the sp^3 protons of triptycene and *t*-butyl at 5.5 and 1.3 ppm, respectively (seeFigures 1 and S3 in the Supporting Information).

Likewise, the ^{13}C NMR spectrum exhibited all the distinctive peaks for **BCM3** including the aromatic carbons in the range of 149.5−123.3 ppm and the three peaks at 52.0, 34.6, and 31.5 ppm, assigned to the sp^3 carbons of the triptycene and *t*-butyl groups (see Figure S9 in the Supporting Information). Likewise, the ^{1}H- and ^{13}C NMR spectra of **BCM1−2** corroborate their successful formation by displaying all of the desired chemical shifts (see Figures S1−S2,S7−S8 in the Supporting Information).

3.2. Synthesis of Copolymers BCP1−3. Scheme 2 depicts the synthetic route to make copolymers **BCP1−3** whose reaction conditions are similar to those utilized to make **BCM1−3** described in Scheme 1 where the reaction of the diethynyl aryl derivatives **2a−c** with 10,10′-dibromo-9,9′-bianthracene **3** resulted in the target copolymers **BCP1−3** in excellent yields (Scheme 2).

The aforementioned polymerization conditions affording **BCP1−3** were obtained only after optimizing the reaction using **2a** and **3** as model comonomers, which consisted of varying the reactants' concentrations and reaction time, while monitoring the molar mass of the resulting product using GPC (Table 1). Initially, a 10^{-1} M solution of an equimolar mixture of 10,10′-dibromo-9,9′-bianthracene **3** and **2a** was reacted at 130 °C in a 1:1 mixture of DMF/toluene for 4 days yielding 98% of **BCP1** whose average weight molar mass (M_w) was found to be 31.5 kDa with a polydispersity index ($Đ$) of 2.5 (Table 1, entry 1). Nevertheless, when the reaction was performed at a lower concentration of **3** and **2a** (i.e., 5.0×10^{-2} M) for the same duration, **BCP1** was obtained in 50% yield with slightly lower average molar mass values (Table 1, entry 2). Likewise, **BCP1** was isolated in a scarce 40% and low molar masses when the concentration of comonomers **3** and **2a** was increased to 2.0×10^{-1} M (Table 1, entry 3). It is noteworthy that starting materials and short oligomer chains were detected in the polymerization attempts shown in entries 2 and 3 of Table 1, thus indicating the possibility to improve both the reaction yield and copolymers' chain growth.

Therefore, maintaining the concentration of **2a** and **3** at 1.0×10^{-1} M but extending the reaction time to 6 days afforded target copolymer **BCP1** quantitatively and in high purity with an average weight molar mass of 61.0 kDa and a polydispersity index ($Đ$) of 2.0 (Table 1, entry 4). The aforementioned optimal reaction conditions were applied to synthesize **BCP2,3** and were isolated in high yields and found to have Mws of 11.0 ($Đ$ = 1.7) and 15.6 kDa ($Đ$ = 1.8), respectively (Table 1, entries 5 and 6). The high purity of copolymers **BCP1−3** was confirmed by various analytical tools, including GPC, ^{1}H- and ^{13}C NMR spectroscopy, FTIR, TGA, UV−vis absorption, and emission spectroscopies (seeFigures 2−5 and S4−S6, S10−S12, S13−S14, S18−S20 in Supporting Information).

Figure 3 displays comparative FT-IR absorption spectra of surrogates **3** and **2c** with that of copolymer **BCP3**. The distinctive stretching vibrations of C−Br in **3**, typically observed at 740 cm^{-1},[17] and those of the alkynyl group (C≡C) in **2c**, detected at 2210 cm^{-1},[37,38] are not spotted in the infrared absorption spectrum of **BCP3**, which proves the formation of the desired cyclopentannulated polymer. Additionally, the IR spectrum of **BCP3** reveals noticeable stretching vibrations of aromatic and aliphatic C−H bonds detected at 3065 and 2963 cm^{-1}, respectively, as well as the bending vibrations of aromatic and aliphatic C−H bonds encountered at 836 and 1438 cm^{-1}, respectively, which further corroborate the successful formation of copolymer **BCP3**.[39,40]

The thermal properties of copolymers **BCP1−3** were examined using TGA, disclosing a pronounced stability as it could be noticed from Figure 4 where the 10% mass loss temperatures of **BCP1,2** were found to be ≥800 °C, whereas that of **BCP3** is detected at 480 °C. Interestingly, the 2% weight loss temperatures of **BCP1,2** were found to be >500

https://doi.org/10.1021/acsomega.3c07108
ACS Omega 2023, 8, 43227−43235

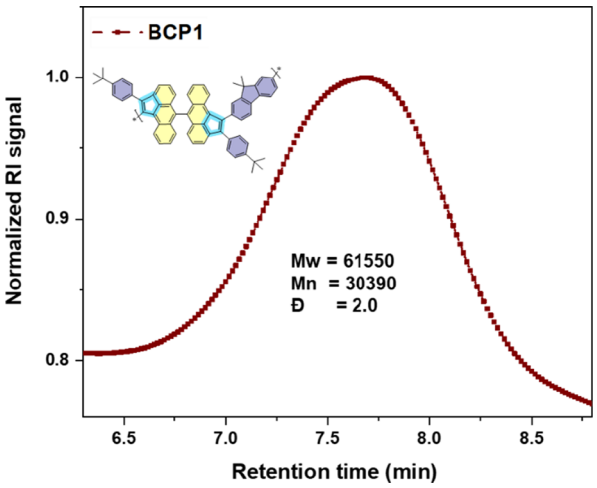

Figure 2. Normalized GPC chromatogram of **BCP1**.

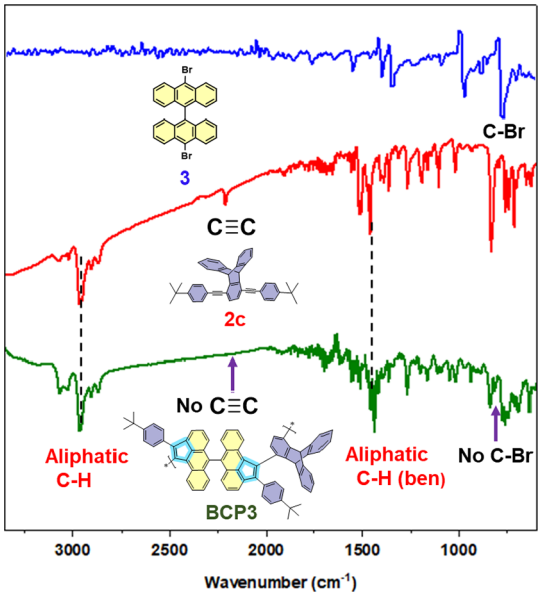

Figure 3. Comparative FT-IR spectra of **3**, **2c**, and **BCP3**.

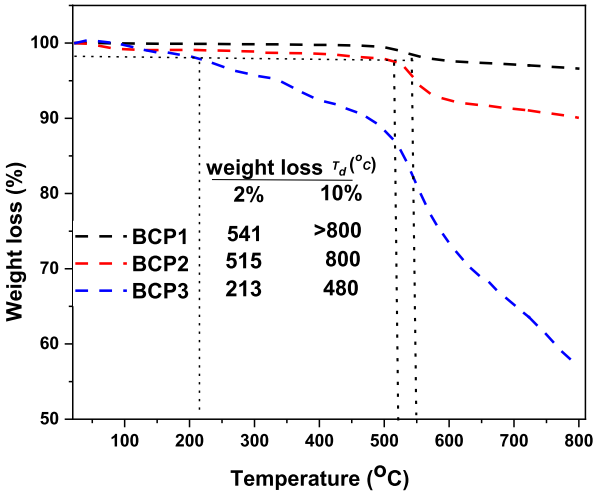

Figure 4. TGA thermograms of copolymers **BCP1−3**. T_d represents the temperature of 2 and 10% weight loss.

°C, thus proving their high thermal stability which can be ascribed to their intricate chemical structures composed of alternating rigid units of the cyclopentannulated aceanthrylenyl units with either fluorene or bifluorene moieties. The high stability of the latter polycondensed aromatic units coupled with the structural rigidity of the interlocked biaceanthrylenyl comonomers render the polymer backbone more resistant to thermal degradation compared to flexible polymers whose increase of rotation with heat leads to their faster degradation.[41] The enhanced thermal stability allows these copolymers to withstand harsh environment of high temperatures without undergoing any significant chemical degradation.

The optical properties of copolymers **BCP1−3** were investigated by UV−vis absorption and emission. **BCP1,2** portrayed analogous UV−vis absorption spectral features, with strong bands observed at 380 and 434 nm, whereas **BCP3**, which contains triptycene units, displays absorption bands at 380, 424, and 452 nm. It is worth noting that all three copolymers display a shoulder peak at 520 nm (Figure 5a). Interestingly, the emission spectra of copolymers **BCP1,3** exhibit a broad band with peak maxima at 410 and 435 nm, respectively. **BCP2**, conversely, shows a sharp emission band whose peak maximum was revealed at 392 nm (Figure 5b).

3.3. Iodine Adsorption Studies. The cyclopentannulated copolymers **BCP1−3** were investigated for their iodine sorption properties, and the experiments consisted of exposing 25 mg of a given copolymer to excess I_2 vapors by placing solid iodine in an open glass vial and confining both the adsorbent and adsorbate inside a sealed glass vessel at 80 °C under atmospheric pressure.[31] Iodine adsorption was measured by recording the amount of iodine at different time intervals using the following equation[31]:

$$M_2\text{-}M_1/M_1 \times 100\%(100\text{wt}\% = 1000\text{mgg}^{-1})$$

where M_2 and M_1 are the masses of the given copolymer after and before iodine uptake, respectively. The results of the gravimetric iodine adsorption experiments are summarized in Table 2. After 6 h of iodine exposure, **BCP2** disclosed an uptake capacity of 1290 mg g^{-1}, while **BCP1** and **BCP3** revealed capacities of 1180 and 1000 mg g^{-1}, respectively (Table 2, entry 8). **BCP2** adsorbed iodine with a capacity of 2900 mg g^{-1} after 72 h of exposure, whereas **BCP1** and **BCP3** attained lower uptake capacities of 1770 and 1240 mg g^{-1}, respectively (Table 2, entry 11) (Figure 6a). Interestingly, the hitherto stated adsorption values did not change even after 72 h, therefore indicating that the copolymers were saturated with iodine. The iodine adsorption capacity recorded for **BCP2** outperforms many copolymers reported in the literature, including nitrogen-abundant covalent organic frameworks (2620 mg g^{-1}),[42] copper-containing zeolites (450 mg g^{-1}),[43] nitrogen-rich thorium nanotube materials (955 mg g^{-1}),[44] metalorganic copolymers (2360 mg g^{-1}),[31] conjugated porous materials (1660 mg g^{-1}),[34] porous carbon materials (955 mg g^{-1}),[45] and conjugated polymers (2000 mg g^{-1}).[21] The adsorbed I2 was desorbed by warming the iodine-loaded copolymers (**BCP1−3@I2**) in air at 125 °C, and the desorption efficiency was calculated at various time periods and found to be quantitative as shown in Figure 6b. It is noteworthy that upon exposure to **BCP1−3** to iodine vapors, the former compounds underwent a color shift from brick red to black and reverted to their original color when heated to desorb iodine (Figure 6a, inset).

https://doi.org/10.1021/acsomega.3c07108
ACS Omega 2023, 8, 43227−43235

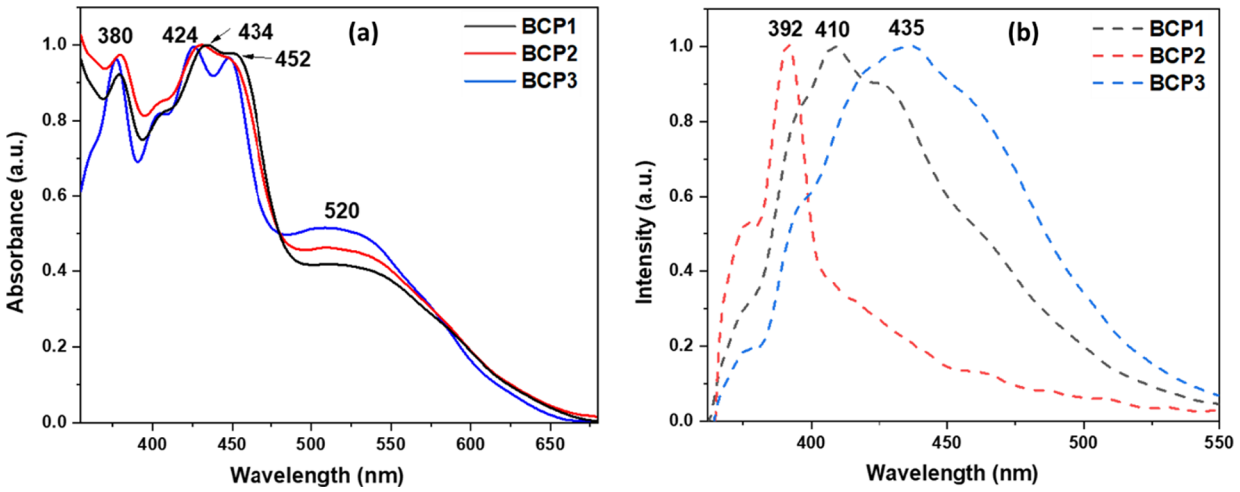

Figure 5. Normalized UV−vis absorption (a) and emission (excitation wavelength λ_{ex} = 350 nm) (b) spectra of **BCP1−3** ($C_M = 10^{-6}$ M in THF).

Table 2. Summary of I_2 Uptake of Copolymers BCP1−3

entry	time[a]	BCP1[b]	BCP2[b]	BCP3[b]
1	0	--	--	--
2	0.5	320	240	240
3	1	450	430	380
4	2	680	670	620
5	3	820	860	760
6	4	950	1050	860
7	5	1090	1190	950
8	6	1180	1290	1000
9	24	1410	2240	1140
10	48	1730	2710	1190
11	72	1770	2900	1240

[a]Hours. [b]Iodine uptake in mg g^{-1}.

Iodine adsorption kinetics by **BCP1−3** were investigated (c.f. Figures 7, S21−S22 and Table 3, S1−S2 in the Supporting Information File) where the pseudo-first-order model is described by the following equation[31]:

$$\ln(q_e - q_t) = \ln q_e - k_1 t$$

whereas the linear expression below was utilized for the pseudo-second-order model[31]:

$$t/q_t = t/q_e + 1/k_2 q_e^2$$

Here, q_t (mg g^{-1}) and q_e (mg g^{-1}) represent the mass of iodine adsorbed per gram adsorbent at time t and at equilibrium, respectively. The rate constants of the pseudo-first-order and pseudo-second-order models are denoted by k_1 and k_2, respectively.[31]

It can be noticed from Figure 7 that the computed iodine adsorption capacity of **BCP2** at equilibrium, $q_{e,cal}$, using the pseudo-first-order model (Figure 7a), was derived from the plot of $\ln(q_e - q_t)$ against time (t) whereas that of the pseudo-second-order model (Figure 7b) was computed from the plot of t/q_t versus time (t). Table 3 clearly reveals that the correlation coefficient (R^2) of 0.9958, which is derived from the linear plot of the pseudo-second-order model, is higher than that determined from the pseudo-first-order model whose value R^2 = 0.9894. The comparison of **BCP2** experimental and calculated iodine uptake capacities at equilibrium, $q_{e,exp}$ and $q_{e,cal}$, respectively, suggests a stronger agreement between the former of 2900 mg g^{-1} and the latter of 3070 mg g^{-1} and which

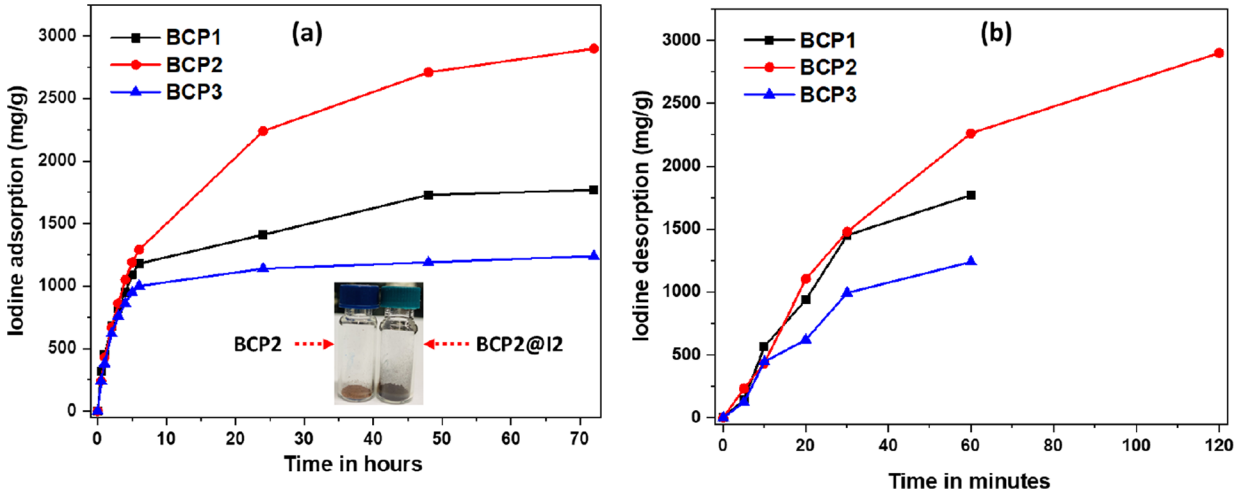

Figure 6. Adsorption (a) at 80 °C and desorption (b) at 125 °C (in air) of I_2 with respect to time. Inset: photographs revealing the color shift after I_2 uptake.

https://doi.org/10.1021/acsomega.3c07108
ACS Omega 2023, 8, 43227−43235

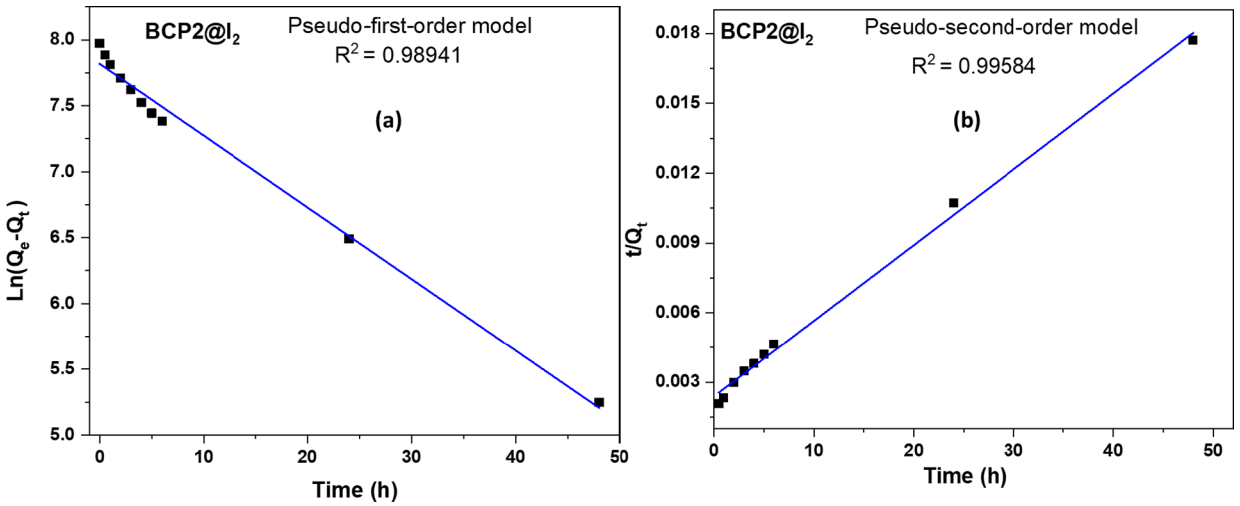

Figure 7. Pseudo-first-order (a) and pseudo-second-order (b) kinetic models of **BCP2@I2**.

Table 3. Pseudo-First-Order and Pseudo-Second-Order Parameters of BCP2@I2

		pseudo-first-order model			pseudo-second-order model		
copolymer	$q_{e,exp}$ (mg g^{-1})	$q_{e,cal}$ (mg g^{-1})	k_1 (h^{-1})	R^2	$q_{e,cal}$ (mg g^{-1})	k_2 (h^{-1})	R^2
BCP2@I2	2900	2484	−0.00175	0.98941	3070	4.44×10^{-05}	0.99584

is extrapolated from the pseudo-second-order model, thus indicating that it is more favored than the pseudo-first-order model. Similarly, copolymers **BCP1** and **BCP3** were also found to follow the pseudo-second-order kinetic model (c.f. Figures S21−S22 and Tables S1−S2 in the Supporting Information).

Desorption experiments were performed to check the reversibility of I_2 uptake by **BCP1−3**. Therefore, the latter was immersed in ethanol—a well-known solvent of iodine, and desorption was investigated by monitoring the ultraviolet−visible absorbance spectra at various time periods (see Figure 8 and S23−S24 in Supporting Information). The absorbance spectra revealed a noticeable increase in the intensity maxima which correspond to I_2 as a function of time, notably, the peaks detected at 228 nm, which is attributed to I_2, as well as the two peaks encountered at ∼289 and ∼360 nm, which are associated with polyiodide ions. This undoubtedly indicates the efficient release of the adsorbed iodine from **BCP1** under ambient conditions, showing a rapid increase within the first 20 min reaching equilibrium after ∼45 min. Additionally, the color of the solution changed from colorless to yellow, thus providing further confirmation of the iodine release from the copolymer into ethanol solution.

The copolymers' reusability tests were investigated using **BCP2** as this latter disclosed the highest iodine uptake property where **BCP2@I2** was warmed at 125 °C for 24 h to make sure of the full release of any adsorbed iodine. The regenerated **BCP2** was then exposed to I_2 vapors, and its uptake capacity was found to be similar to that of a freshly prepared polymer (Table 2). This regeneration procedure was repeated for five consecutive cycles, and the iodine adsorption efficiency of the regenerated **BCP2** sample showed only a minor decrease of ∼3.5% throughout the entire set of experiments (Figure 9), which strongly supports the possibility to use **BCP1−3** copolymers as effective sorbent materials to

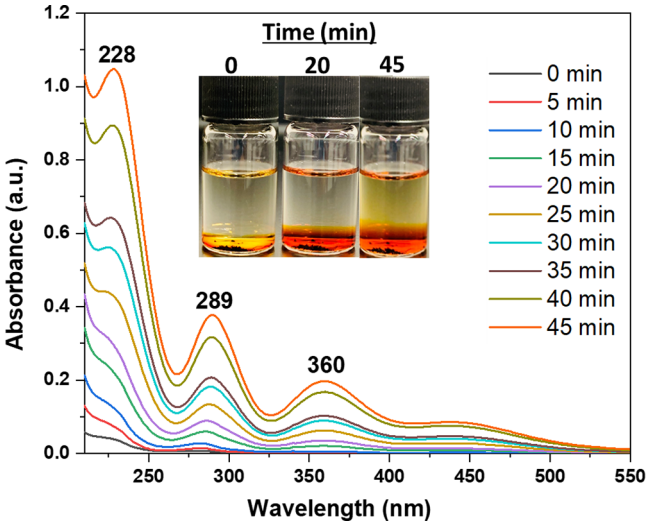

Figure 8. UV−vis absorption spectra upon immersion of **BCP1@I2** in ethanol. Inset: photos of the solutions showing the color change upon immersion in ethanol.

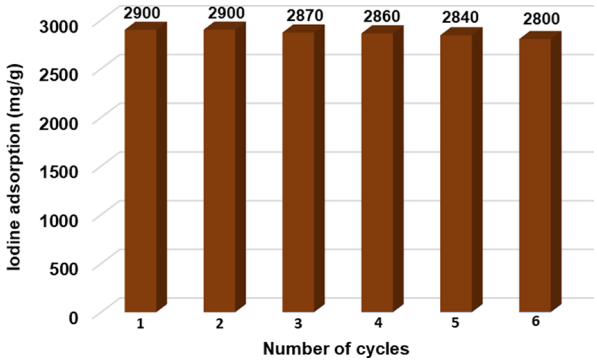

Figure 9. Graphical representation of iodine capture recyclability by **BCP2**.

https://doi.org/10.1021/acsomega.3c07108
ACS Omega 2023, 8, 43227−43235

capture iodine vapors even after several usages. It should be noted that regeneration of the polymers loaded with iodine (**BCP1−3@I2**) can be carried out via two options, either by warming them in open air or by soaking the polymers in ethanol.

4. CONCLUSIONS

New conjugated copolymer structures, **BCP1−3**, were made in high yield using a versatile [3 + 2] cyclopolymerization reaction. These polymers, which bear alternating comonomers of the interlocked 6,6′-biaceanthrylenyl moieties with various spiro units, namely, dimethyl fluorene (**BCP1**), spirobifluorene (**BCP2**), and triptycene (**BCP3**), exhibited high relative weight-average molecular weights (M_w) ranging from 11.0 to 61.5 kg mol^{-1} and a polydispersity index ($Đ = M_w/M_n$) that ranges from 1.7 to 2.0. The intricate structures of **BCP1−3** bestowed them with remarkable thermal stability with 10% weight loss observed at temperatures exceeding 800 °C. Iodine sorption studies of **BCP1−3** not only demonstrated their exceptional uptake capacity reaching 2900 mg g^{-1} for **BCP2** but also revealed it to be easily regenerated either by heating them in ambient air or by immersing them in ethanol. The properties of these highly stable materials promote them as promising I_2 adsorbents for applications in environmental remediation under extreme thermal conditions.

■ ASSOCIATED CONTENT

Data Availability Statement

The raw data required to reproduce these findings are available upon request.

Supporting Information

The Supporting Information is available free of charge at https://pubs.acs.org/doi/10.1021/acsomega.3c07108.

^{1}H and ^{13}C NMR and FTIR spectra of **BCM1−3** and **BCP1−3**; GPC chromatograms of **BCP2−3**; kinetic models and kinetic parameters of **BCP1@I2** and **BCP3@I2**; and iodine desorption of **BCP2@I2** and **BCP3@I2** in ethanol (PDF)

■ AUTHOR INFORMATION

Corresponding Author

Bassam Alameddine − *Department of Mathematics and Natural Sciences and Functional Materials Group, Gulf University for Science and Technology, Hawally 32093, Kuwait;* orcid.org/0000-0002-7881-4392; Phone: +965 2530 7111; Email: alameddine.b@gust.edu.kw

Authors

Noorullah Baig − *Department of Mathematics and Natural Sciences and Functional Materials Group, Gulf University for Science and Technology, Hawally 32093, Kuwait;* orcid.org/0000-0002-9193-1171

Suchetha Shetty − *Department of Mathematics and Natural Sciences and Functional Materials Group, Gulf University for Science and Technology, Hawally 32093, Kuwait*

Rupa Bargakshatriya − *CSIR-Central Salt and Marine Chemicals Research Institute, Bhavnagar, Gujarat 364002, India*

Sumit Kumar Pramanik − *CSIR-Central Salt and Marine Chemicals Research Institute, Bhavnagar, Gujarat 364002, India;* orcid.org/0000-0002-0294-8829

Complete contact information is available at: https://pubs.acs.org/10.1021/acsomega.3c07108

Notes

The authors declare no competing financial interest.

■ ACKNOWLEDGMENTS

The project was partially supported by the Kuwait Foundation for the Advancement of Sciences (KFAS) under project code PN18-14SC-03.

■ REFERENCES

(1) Haque, A.; Alenezi, K. M.; Khan, M. S.; Wong, W.-Y.; Raithby, P. R. Non-covalent interactions (NCIs) in π-conjugated functional materials: advances and perspectives. *Chem. Soc. Rev.* **2023**, *52* (2), 454−472.

(2) Lee, J.-S. M.; Cooper, A. I. Advances in Conjugated Microporous Polymers. *Chem. Rev.* **2020**, *120* (4), 2171−2214.

(3) Giri, D.; Saha, S. K.; Siemons, N.; Anderson, I.; Yu, H.; Nelson, J.; Canjeevaram Balasubramanyam, R. K.; Patil, S. Ion Size-Dependent Electrochromism in Air-Stable Napthalenediimide-Based Conjugated Polymers. *ACS Appl. Mater. Interfaces* **2023**, *15* (14), 17767−17778.

(4) Li, S.; Zhou, Y.; Hu, Z.; Meng, X.; Shi, H.; Zhang, X.; Hou, G.; Zhu, J.; Wang, J. Green and Sustainable Hydroxyquinone Molecule Electrodes Prepared for Efficient Energy Storage. *ACS Appl. Energy Mater.* **2023**, *6* (9), 4788−4799.

(5) Amin, K.; Ashraf, N.; Mao, L.; Faul, C. F. J.; Wei, Z. Conjugated microporous polymers for energy storage: Recent progress and challenges. *Nano Energy* **2021**, *85*, No. 105958.

(6) Schon, T. B.; McAllister, B. T.; Li, P.-F.; Seferos, D. S. The rise of organic electrode materials for energy storage. *Chem. Soc. Rev.* **2016**, *45* (22), 6345−6404.

(7) Ko, J.; Berger, R.; Lee, H.; Yoon, H.; Cho, J.; Char, K. Electronic effects of nano-confinement in functional organic and inorganic materials for optoelectronics. *Chem. Soc. Rev.* **2021**, *50* (5), 3585−3628.

(8) Anderson, C. L.; Zhang, T.; Qi, M.; Chen, Z.; Yang, C.; Teat, S. J.; Settineri, N. S.; Dailing, E. A.; Garzón-Ruiz, A.; Navarro, A.; Lv, Y.; Liu, Y. Exceptional Electron-Rich Heteroaromatic Pentacycle for Ultralow Band Gap Conjugated Polymers and Photothermal Therapy. *J. Am. Chem. Soc.* **2023**, *145* (9), 5474−5485.

(9) Bell, K.-J. J.; Kisiel, A. M.; Smith, E.; Tomlinson, A. L.; Collier, G. S. Simple Synthesis of Conjugated Polymers Enabled via Pyrrolo[3,2-b]pyrroles. *Chem. Mater.* **2022**, *34* (19), 8729−8739.

(10) Zhang, D.-W.; Li, M.; Chen, C.-F. Recent advances in circularly polarized electroluminescence based on organic light-emitting diodes. *Chem. Soc. Rev.* **2020**, *49* (5), 1331−1343.

(11) Wei, X.; Pan, Y.; Zhang, W.; Zhou, Y.; Li, H.; Wang, L.; Yu, G. Incorporation of the Benzobisthiadiazole Unit Leads to Open-Shell Conjugated Polymers with n-Type Charge Transport Properties. *Macromolecules* **2023**, *56* (8), 2980−2989.

(12) Baig, N.; Shetty, S.; Fall, S.; Al-Mousawi, S.; Heiser, T.; Alameddine, B. Conjugated copolymers bearing 2,7-dithienylphenanthrene-9,10-dialkoxy units: highly soluble and stable deep-blue emissive materials. *New J. Chem.* **2020**, *44* (22), 9557−9564.

(13) Shetty, S.; Baig, N.; Bargakshatriya, R.; Pramanik, S. K.; Alameddine, B. High Uptake of the Carcinogenic Pararosaniline Hydrochloride Dye from Water Using Carbazole-Containing Conjugated Copolymers Synthesized from a One-Pot Cyclopentannulation Reaction. *ACS Appl. Mater. Interfaces* **2023**, *15*, 28149−28157.

(14) Du, Y.; Lovell, H. B.; Lirette, F.; Morin, J.-F.; Plunkett, K. N. Electron Acceptors Based on Cyclopentannulated Anthanthrenes. *J. Org. Chem.* **2021**, *86* (2), 1456−1461.

(15) Lütke Eversloh, C.; Avlasevich, Y.; Li, C.; Müllen, K. Palladium-Catalyzed Pentannulation of Polycyclic Aromatic Hydrocarbons. *Chem. -Eur. J.* **2011**, *17* (45), 12756−12762.

(16) Bheemireddy, S. R.; Hussain, W. A.; Uddin, A.; Du, Y.; Hautzinger, M. P.; Kevorkian, P. V.; Petrie, F. A.; Plunkett, K. N.

Cyclopentannulation and cyclodehydrogenation of isomerically pure 5,11-dibromo-anthradithiophenes leading to contorted aromatics. *Chem. Commun.* **2018**, *54* (100), 14140−14143.
(17) Baig, N.; Shetty, S.; Tiwari, R.; Pramanik, S. K.; Alameddine, B. Aggregation-Induced Emission of Contorted Polycondensed Aromatic Hydrocarbons Made by Edge Extension Using a Palladium-Catalyzed Cyclopentannulation Reaction. *ACS Omega* **2022**, *7* (49), 45732−45739.
(18) Bheemireddy, S. R.; Hautzinger, M. P.; Li, T.; Lee, B.; Plunkett, K. N. Conjugated Ladder Polymers by a Cyclopentannulation Polymerization. *J. Am. Chem. Soc.* **2017**, *139* (16), 5801−5807.
(19) Uddin, A.; Plunkett, K. N. Donor-acceptor copolymers from cyclopentannulation polymerizations with dicyclopenta[cd,jk]pyrene and dicyclopenta[cd,lm] perylene acceptors. *J. Polym. Sci.* **2020**, *58* (22), 3165−3169.
(20) Zhu, X.; Bheemireddy, S. R.; Sambasivarao, S. V.; Rose, P. W.; Torres Guzman, R.; Waltner, A. G.; DuBay, K. H.; Plunkett, K. N. Construction of Donor−Acceptor Polymers via Cyclopentannulation of Poly(arylene ethynylene)s. *Macromolecules* **2016**, *49* (1), 127−133.
(21) Baig, N.; Shetty, S.; Al-Mousawi, S.; Alameddine, B. Synthesis of conjugated polymers via cyclopentannulation reaction: promising materials for iodine adsorption. *Polym. Chem.* **2020**, *11* (17), 3066−3074.
(22) Pan, T.; Yang, K.; Dong, X.; Han, Y. Adsorption-based capture of iodine and organic iodides: status and challenges. *J. Mater. Chem. A* **2023**, *11* (11), 5460−5475.
(23) Das, S.; Heasman, P.; Ben, T.; Qiu, S. Porous Organic Materials: Strategic Design and Structure−Function Correlation. *Chem. Rev.* **2017**, *117* (3), 1515−1563.
(24) Wan, N.; Chang, Q.; Hou, F.; Zhang, S.; Zang, X.; Zhao, X.; Wang, C.; Wang, Z.; Yamauchi, Y. Nanoarchitectured Conjugated Microporous Polymers: State of the Art Synthetic Strategies and Opportunities for Adsorption Science. *Chem. Mater.* **2022**, *34* (17), 7598−7619.
(25) Liu, S.-N.; Wang, H.-N.; Feng, M.-L.; Yang, K.-L.; Cai, S.; Fan, J.; Zhang, W.-G.; Zheng, S.-R. Metal−Organic Cage Extended Amorphous Network via Anionic Organic Linkers for Cr2O72− and Iodine Adsorption on Nanopores. *ACS Appl. Nano Mater.* **2023**, *6* (1), 656−663.
(26) Li, H.; Zhang, D.; Cheng, K.; Li, Z.; Li, P.-Z. Effective Iodine Adsorption by Nitrogen-Rich Nanoporous Covalent Organic Frameworks. *ACS Appl. Nano Mater.* **2023**, *6* (2), 1295−1302.
(27) Zhang, X.; Maddock, J.; Nenoff, T. M.; Denecke, M. A.; Yang, S.; Schröder, M. Adsorption of iodine in metal−organic framework materials. *Chem. Soc. Rev.* **2022**, *51* (8), 3243−3262.
(28) Yildirim, O.; Tsaturyan, A.; Damin, A.; Nejrotti, S.; Crocellà, V.; Gallo, A.; Chierotti, M. R.; Bonomo, M.; Barolo, C. Quinoid-Thiophene-Based Covalent Organic Polymers for High Iodine Uptake: When Rational Chemical Design Counterbalances the Low Surface Area and Pore Volume. *ACS Appl. Mater. Interfaces* **2023**, *15* (12), 15819−15831.
(29) Hassan, A.; Alam, A.; Ansari, M.; Das, N. Hydroxy functionalized triptycene based covalent organic polymers for ultra-high radioactive iodine uptake. *Chem. Eng. J.* **2022**, *427*, No. 130950.
(30) Prince, A.; Hassan, S.; Chandra, A.; Alam, N. Das, Super-fast iodine capture by an ionic covalent organic network (iCON) from aqueous and vapor media. *RSC Sustain.* **2023**, *1* (3), 511−522.
(31) Baig, N.; Shetty, S.; Habib, S. S.; Husain, A. A.; Al-Mousawi, S.; Alameddine, B. Synthesis of Iron(II) Clathrochelate-Based Poly(vinylene sulfide) with Tetraphenylbenzene Bridging Units and Their Selective Oxidation into Their Corresponding Poly(vinylene sulfone) Copolymers: Promising Materials for Iodine Capture. *Polymers (Basel)* **2022**, *14* (18), 3727.
(32) Shetty, S.; Baig, N.; Alameddine, B. Synthesis and Iodine Adsorption Properties of Organometallic Copolymers with Propeller-Shaped Fe(II) Clathrochelates Bridged by Different Diaryl Thioether and Their Oxidized Sulfone Derivatives. *Polymers* **2022**, *14* (22), 4818.
(33) Hassan, A.; Alam, A.; Chandra, S.; Prince, N. Das, Triptycene-based and imine linked porous uniform microspheres for efficient and reversible scavenging of iodine from various media: a systematic study. *Environ. Sci.: Adv.* **2022**, *1* (3), 320−330.
(34) Baig, N.; Shetty, S.; Al-Mousawi, S.; Alameddine, B. Conjugated microporous polymers using a copper-catalyzed [4 + 2] cyclobenzannulation reaction: promising materials for iodine and dye adsorption. *Polym. Chem.* **2021**, *12* (15), 2282−2292.
(35) Luo, D.; He, Y.; Tian, J.; Sessler, J. L.; Chi, X. Reversible Iodine Capture by Nonporous Adaptive Crystals of a Bipyridine Cage. *J. Am. Chem. Soc.* **2022**, *144* (1), 113−117.
(36) Baig, N.; Shetty, S.; Al-Mousawi, S.; Al-Sagheer, F.; Alameddine, B. Synthesis of triptycene-derived covalent organic polymer networks and their subsequent in-situ functionalization with 1,2-dicarbonyl substituents. *React. Funct. Polym.* **2019**, *139*, 153−161.
(37) Shetty, S.; Baig, N.; Hassan, A.; Al-Mousawi, S.; Das, N.; Alameddine, B. Fluorinated Iron(ii) clathrochelate units in metal-organic based copolymers: improved porosity, iodine uptake, and dye adsorption properties. *RSC Adv.* **2021**, *11* (25), 14986−14995.
(38) Shetty, S.; Baig, N.; Al-Mousawi, S.; Alameddine, B. Removal of anionic and cationic dyes using porous copolymer networks made from a Sonogashira cross-coupling reaction of diethynyl iron (II) clathrochelate with various arylamines. *J. Appl. Polym. Sci.* **2022**, *139* (43), No. e52966.
(39) Alameddine, B.; Baig, N.; Shetty, S.; Al-Mousawi, S. Conjugated copolymers bearing 2,7-di(thiophen-2-yl)phenanthrene-9,10-dione units and alteration of their emission via functionalization of the ortho-dicarbonyl groups into quinoxaline and phenazine derivatives. *Polymer* **2019**, *178*, No. 121589.
(40) Baig, N.; Shetty, S.; Pasha, S. S.; Pramanik, S. K.; Alameddine, B. Copolymer networks with contorted units and highly polar groups for ultra-fast selective cationic dye adsorption and iodine uptake. *Polymer* **2022**, *239*, No. 124467.
(41) Cai, Y.; Lu, J.; Jing, G.; Yang, W.; Han, B. High-Glass-Transition-Temperature Hydrocarbon Polymers Produced through Cationic Cyclization of Diene Polymers with Various Microstructures. *Macromolecules* **2017**, *50* (19), 7498−7508.
(42) Cheng, K.; Li, H.; Li, Z.; Li, P.-Z.; Zhao, Y. Linking Nitrogen-Rich Organic Cages into Isoreticular Covalent Organic Frameworks for Enhancing Iodine Adsorption Capability. *ACS Mater. Lett.* **2023**, *5* (6), 1546−1555.
(43) Zhou, J.; Chen, Q.; Li, T.; Lan, T.; Bai, P.; Liu, F.; Yuan, Z.; Zheng, W.; Yan, W.; Yan, T. Porous Copper-Loaded Zeolites for High-Efficiency Capture of Iodine from Spent Fuel Reprocessing Off-Gas. *Inorg. Chem.* **2022**, *61* (20), 7746−7753.
(44) Hastings, A. M.; Ray, D.; Hanna, S. L.; Jeong, W.; Chen, Z.; Oliver, A. G.; Gagliardi, L.; Farha, O. K.; Hixon, A. E. Leveraging Nitrogen Linkages in the Formation of a Porous Thorium−Organic Nanotube Suitable for Iodine Capture. *Inorg. Chem.* **2022**, *61* (25), 9480−9492.
(45) Yin, Y.; Liang, D.; Liu, D.; Liu, Q. Preparation and characterization of three-dimensional hierarchical porous carbon from low-rank coal by hydrothermal carbonization for efficient iodine removal. *RSC Adv.* **2022**, *12* (5), 3062−3072.

https://doi.org/10.1021/acsomega.3c07108
ACS Omega 2023, 8, 43227−43235